J Mater Sci (2009) 44:1344–1350
DOI 10.1007/s10853-008-3012-4

Characterization and biological application of YAG:Ce^{3+} nanophosphor modified with mercaptopropyl trimethoxy silane

Atsushi Tsukamoto · Tetsuhiko Isobe

Received: 16 June 2008 / Accepted: 17 September 2008 / Published online: 8 October 2008

Abstract We focus on the inorganic nanophosphor of YAG:Ce^{3+} nanoparticles as an alternative fluorescent probe instead of organic dyes for biological application. YAG:Ce^{3+} nanoparticles have the green emission at 530 nm under the excitation of blue light at 450 nm. Conventional biochemical equipments for organic dyes can be used for YAG:Ce^{3+} nanoparticles. SH groups were introduced by surface modification of YAG:Ce^{3+} nanoparticles with 3-mercaptopropyl trimethoxy silane, and were characterized by X-ray fluorescence analysis, FT-IR, and Ellman method. We demonstrated tagging avidin-immobilized agarose gel beads with biotinylated-YAG:Ce^{3+} nanoparticles, and tagging rabbit IgG-immobilized agarose gel beads with antirabbit IgG-immobilized YAG:Ce^{3+} nanoparticles.

Abbreviations

YAG:Ce^{3+}	Yttrium aluminum garnet doped with Ce^{3+}
APTMS	3-Aminopropyl trimethoxy silane
MPTMS	3-Mercaptopropyl trimethoxy silane
1,4-BD	1,4-Butanediol
EMCS	*n*-(6-Maleimidocaproyloxy) sulfosuccinimide
DTNB	5,5′-Dithio-bis-2-nitrobenzoic acid
TNB	5-Thio-2-nitrobenzoic acid
XRF	X-ray fluorescence analysis
UV–vis	Ultraviolet–visible
PL	Photoluminescence
PLE	Photoluminescence excitation
DLS	Dynamic light scattering method

A. Tsukamoto · T. Isobe (✉)
Department of Applied Chemistry, Faculty of Science and Technology, Keio University, 3-14-1 Hiyoshi, Kohoku-ku, Yokohama 223-8522, Japan
e-mail: isobe@applc.keio.ac.jp

Introduction

Development of highly sensitive, nontoxic, nonisotopic analysis systems for biological applications are required in the fields of chemistry, biology, and medical science [1]. Fluorescent labeling for visual analysis of biomolecules and proteins using small organic dyes is widely employed in the life science including diagnostics and biological imaging [1, 2]. Organic dyes, however, have disadvantages such as photodegradation under continuous excitation of light and the overlapped spectra between excitation and emission (narrow Stoke shift), which limit their effectiveness for biological applications [1, 3]. Therefore, it is highly desirable to develop new fluorescent probes for biochemical assays.

Most of the works have reported luminescent semiconductor nanocrystals (called "quantum dots" or QDs) as the phosphore is replaced with organic dyes. They have overcome some of the functional limitations encountered by organic dyes in biotechnological applications. QDs are bright fluorophores that have a broad excitation spectrum and a narrow, symmetric emission spectrum, optical multiplexing, controllable surface properties, and moreover, QDs are highly resistant to photodegradation [4–8]. QDs also have long fluorescence lifetimes in the order of 20–50 ns, which may allow them to be distinguished from background and other fluorophores for increased sensitivity of detection [4]. However, fluorescent QDs probes are used for limited applications, because of high cytotoxity of cadmium (from cadmium chalcogenide-based QD) or lead

(from lead chalcogenide-based QD) [9]. The cytotoxity of QDs may be connected to photochemical processes under the aqueous aerobic conditions of in vitro cell imaging [10]. The process may involve electron transfer from the excited QDs to O_2 to produce superoxide (O^{2-}) and an unpaired hole in the QD [10–12], which can induce ligand oxidation and the corrosion of the nanoparticle outer surface [10, 13]. Alternatively, or concurrently, in the case of cadmium-based QDs, the cytotoxicity is attributed to the release of highly toxic free Cd^{2+} ions, and then killed cells [14–16]. Thus, a direct way to avoid the possible toxicity of QDs is to make them well-coated to become biologically inert. Low or nontoxic organic molecules/polymers (e.g. PEG) or inorganic layers (e.g. ZnS and silica) are chosen as coating materials [9]. While mercaptopropionic acid (MPA)- and polymer-coated nanoparticles showed acute cytotoxic effects at 0.65 and 0.80 μM, respectively, silica-coated QDs showed no cytotoxic effects in the cell lines investigated with concentrations as high as 30 μM [17, 18]. Silanization of various metal and semiconductor nanoparticle system has shown great success in protecting their surface characteristics and functionalizing their surface for biological applications. Silica modification has been shown to provide some prime advantages necessary for bioconjugation of nanoparticle. First the silica shell prevents flocculation of particles, prevents species from adsorbing onto the surface, and helps to improve the photoluminescence. Second, use of the silica shell with functional groups such as thiol, amine, phosphate, carboxylate, and PEG groups enables us to control conjugation protocol [18].

QDs are also used for limited bioimaging because they require harmful UV light for excitation. Therefore, in this work, we focus on YAG:Ce^{3+} nanocrystal phosphor with the following potential in biological applications:

1. YAG:Ce^{3+} can be excited by blue light, which causes less damage to living cells than UV light;
2. YAG:Ce^{3+} nanocrystal phosphor has a luminescence quantum efficiency as high as 20–40% [19], because of the allowed 4f → 5d transition of Ce^{3+} [20];
3. YAG:Ce^{3+} is regarded as a nontoxic biological material.

Asakura et al. [21] have already reported successful biological application of YAG:Ce^{3+} nanoparticles modified with APTMS and conjugated with biotin for specific labeling of avidin-immobilized agarose gel beads .

In this work, we focused on the introduction of SH groups onto the surface of the YAG:Ce^{3+} nanoparticles by surface modification with MPTMS. Then, biological imaging was demonstrated by tagging agarose gel beads with either biotinylated or antibody-immobilized YAG:Ce^{3+} nanoparticles, as shown in Fig. 1. SH groups of the MPTMS-modified YAG:Ce^{3+} nanoparticles are cross-linked with biomolecules (biotin and avidin) using EMCS. SH groups were chosen in this work for three main reasons: (i) high reactivity, (ii) in the case of nanoparticles with NH_2 groups, binding among nanoparticles and among proteins can compete with the conjugation between a particle and a protein. However, a nanoparticle with free SH groups is selectively cross-linked with a protein to form a conjugation between a nanoparticle and a biomolecule because of many proteins with no SH groups. (iii) Many thiolate derivatization reagents have been marketed.

Experimental

Chemicals and materials

Yttrium acetate tetrahydrate (99.99%), cerium acetate hydrate (99.99%), aluminum isopropoxide (99.9%), and 1,4-butanediol (1,4-BD) (97.0%) were purchased from Kanto Chemical. MPTMS was purchased from Aldrich. Biotin-PEO-Amine was purchased from Pierce. Avidin was purchased from Nacalai Tesque. Biotinylated antirabbit IgG, avidin-immobilized agarose gel beads, and rabbit IgG-immobilized agarose gel beads were purchased from Sigma.

Synthesis of YAG:Ce^{3+} nanoparticles by glycothermal method

YAG:Ce^{3+} nanoparticles were synthesized by the previously reported glycothermal method [19, 21, 22]. A mixture of yttrium acetate tetrahydrate (2.5014 g), cerium acetate hydrate (0.0251 g), aluminum isopropoxide (2.553 g), and 1,4-BD (63.6 mL) were poured into a 120-mL autoclave (Taiatsu Techno TVS-120-N2). The sealed autoclave was linearly heated from 25 °C to 300 °C for 90 min with stirring at 300 rpm, kept at the same temperature for 2 h, and cooled to room temperature to obtain the YAG:Ce^{3+} colloidal 1,4-BD solution. This solution was left over 1 week to induce the sedimentation of aggregated particles. The supernatant colloidal 1,4-BD solution was used for conjugation with biomolecules.

Surface modification by MPTMS

YAG:Ce^{3+} nanoparticles were silanized with MPTMS. MPTMS (1 mL) was poured into the YAG:Ce^{3+} colloidal 1,4-BD solution (5 mL). The solution was sonicated for 10 min, set in silicone oil bath, and stirred for 6 h at 65 °C. Then, absolute ethanol (5 mL) was added to the solution, the mixture was sonicated for 10 min. Obtained MPTMS-modified YAG:Ce^{3+} nanoparticles were separated from the solution by centrifugation at 12,000 rpm for 10 min, washed twice with water, and resuspended in ultrapure water (10 mL).

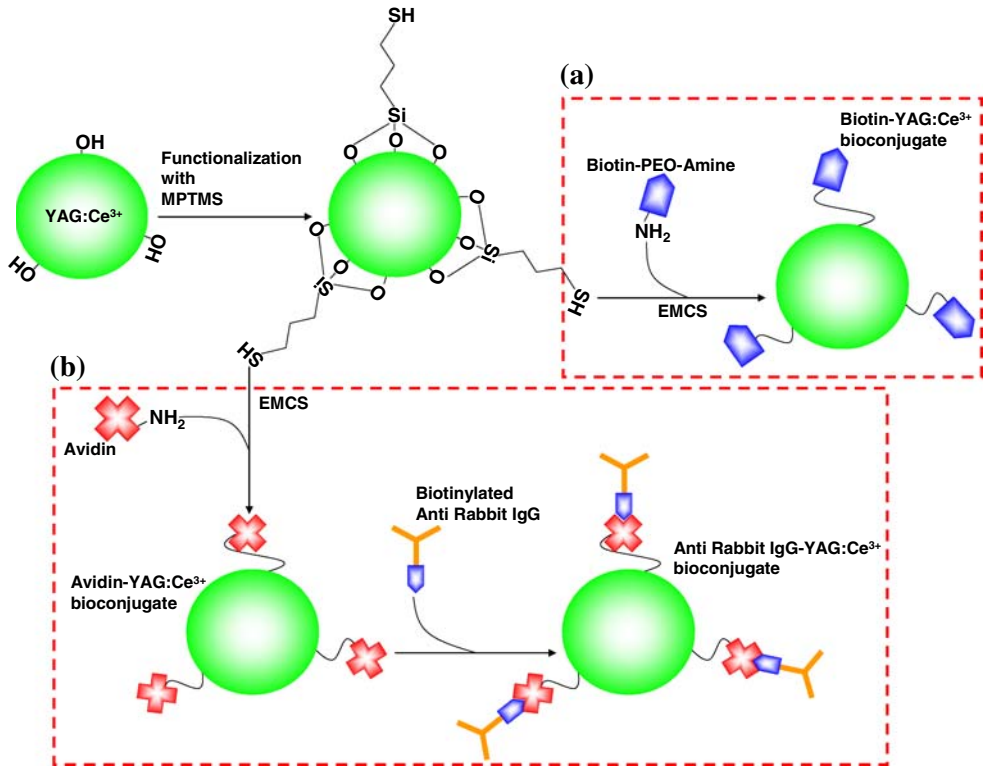

Fig. 1 Schematic illustration showing the biofunctionalization of YAG:Ce^{3+} nanoparticles with biotin or avidin. YAG:Ce^{3+} nanoparticles were first modified with MPTMS, and SH groups introduced on the surface of the nanoparticles were then activated by EMCS to conjugate biotin (**a**) or avidin (**b**). Avidin-immobilized YAG:Ce^{3+} nanoparticles were also immobilized on antirabbit IgG

Biotinylation

The resultant MPTMS-modified YAG:Ce^{3+} nanoparticles were conjugated with biotin using EMCS as a cross-linker. One mg/mL Biotin-PEO-Amine/PBS (1 mL) and 10 mg/mL EMCS/DMSO (0.5 mL) were poured into MPTMS-modified YAG:Ce^{3+} colloidal aqueous solution (10 mL). After stirring for 2 h, obtained biotinylated-YAG:Ce^{3+} nanoparticles were separated from the solution by centrifugation at 12,000 rpm for 10 min, washed three times with water, and resuspended in ultrapure water (10 mL). Then, avidin-immobilized agarose gel beads (0.05 mL) and biotinylated-YAG:Ce^{3+} colloidal aqueous solution (0.2 mL) were poured into ultrapure water (3 mL). After stirring for 2 h, the suspension was moved to ultrafiltration tube. Obtained biotinylated-YAG:Ce^{3+}/avidin-beads complexes were separated from the suspension by centrifugation at 6,300 rpm for 30 s, washed three times with PBS, and resuspended in PBS (0.5 mL).

Antibody immobilization

On the other hand, MPTMS-modified YAG:Ce^{3+} nanoparticles were also conjugated with avidin by the same method, and antibody was subsequently immobilized to the nanoparticles. One mg/mL avidin/PBS (0.5 mL) and 10 mg/mL EMCS/DMSO (0.5 mL) were poured into MPTMS-modified YAG:Ce^{3+} colloidal aqueous solution (10 mL). After stirring for 2 h, obtained avidin-immobilized YAG:Ce^{3+} nanoparticles were separated from the solution by centrifugation at 12,000 rpm for 10 min, washed three times with water, resuspended in ultrapure water (10 mL), and then biotinylated-antirabbit IgG/PBS (0.5 mL) was added to the solution. After stirring for 2 h, obtained antirabbit IgG-immobilized YAG:Ce^{3+} nanoparticles were separated from the solution by centrifugation at 12,000 rpm for 10 min, washed three times with water, and resuspended in ultrapure water (10 mL). Then, rabbit IgG-immobilized agarose gel beads (0.05 mL) and antirabbit IgG-immobilized YAG:Ce^{3+} colloidal aqueous solution (0.2 mL) were poured into ultrapure water (3 mL). After stirring for 2 h, the suspension was moved to ultrafiltration tube. Obtained antirabbit IgG-immobilized YAG:Ce^{3+}/rabbit IgG-bead complexes were separated from the solution by centrifugation at 6,300 rpm for 30 s, washed three times with PBS, and resuspended in PBS (0.5 mL).

Characterization

The composition of the powdered samples of YAG:Ce^{3+} and MPTMS-modified YAG:Ce^{3+} nanoparticles were

investigated by XRF (Rigaku, ZSX mini II). The S–H stretching vibration was investigated by FT-IR spectroscopy (BioRad, FTS-60A) using the diffuse reflectance method. UV–vis spectra were measured by an optical absorption spectrometer (Jasco, V-570) to quantify freely accessible SH groups on the surface of MPTMS-modified YAG:Ce^{3+} nanoparticles by the Ellman method [23], because Ellman's reagent, DTNB, cannot penetrate siloxane network. DTNB reacts with a free S–H group to yield a mixed disulfide and yellow-colored TNB. The molar extinction coefficient of TNB was reported to be 13,600 M^{-1} cm^{-1} at 412 nm at pH 8.0. The absorbance, A, is defined as follows: $A = \varepsilon bc$ where ε = molar extinction coefficient (13,600 M^{-1} cm^{-1}), b = cuvette path length in centimeters (1 cm), c = concentration in moles/liter. A DTNB solution was prepared by dissolving DTNB (4 mg) in PBS (4 mL). MPTMS-modified YAG:Ce^{3+} colloidal aqueous solution (0.25 mL) was poured into a mixture of the DTNB solution (0.05 mL) and PBS (2.5 mL). After stirring for 15 min, the mixture was moved to ultrafiltration tube, and centrifuged at 6,300 rpm for 30 s to remove MPTMS-modified YAG:Ce^{3+} nanoparticles. Then, the mixture (0.5 mL) was diluted to ultrapure water (2.5 mL), and its absorbance at 412 nm was measured to obtain the concentration of TNB, leading to the determination of the amount of free SH groups on the surface. PL and PLE spectra of YAG:Ce^{3+} modified with and without MPTMS colloidal aqueous solutions were measured at room temperature by a fluorescence spectrometer (Jasco, FP-6500) equipped a 150 W Xe lamp and a photomultiplier detector. The size distributions of YAG:Ce^{3+} and MPTMS-modified YAG:Ce^{3+} nanoparticles in aqueous solutions were measured by DLS (Malvern, HPPS). Agarose gel beads tagged with biotinylated-YAG:Ce^{3+} and antirabbit IgG-immobilized YAG:Ce^{3+} nanoparticles were observed by fluorescence microscopy (Nicon, Eclipse, E600) with the excitation wavelength, 430 ± 5 nm; the emission wavelength, 535 ± 20 nm.

Results and discussion

Confirmation of SH groups introduced to YAG:Ce^{3+} nanoparticles

Figure 2 shows the XRF profiles of YAG:Ce^{3+} nanoparticles with and without MPTMS modification. The peaks corresponding to S Kα-line and Si Kα-line from MPTMS were detected at 75.780° and 109.045°, respectively, for MPTMS-modified YAG:Ce^{3+} nanoparticles, whereas both peaks were not detected for unmodified YAG:Ce^{3+} nanoparticles. The molar ratio of Y:S:Si of the MPTMS-modified YAG:Ce^{3+} nanoparticles were 3×10^3:3:2,

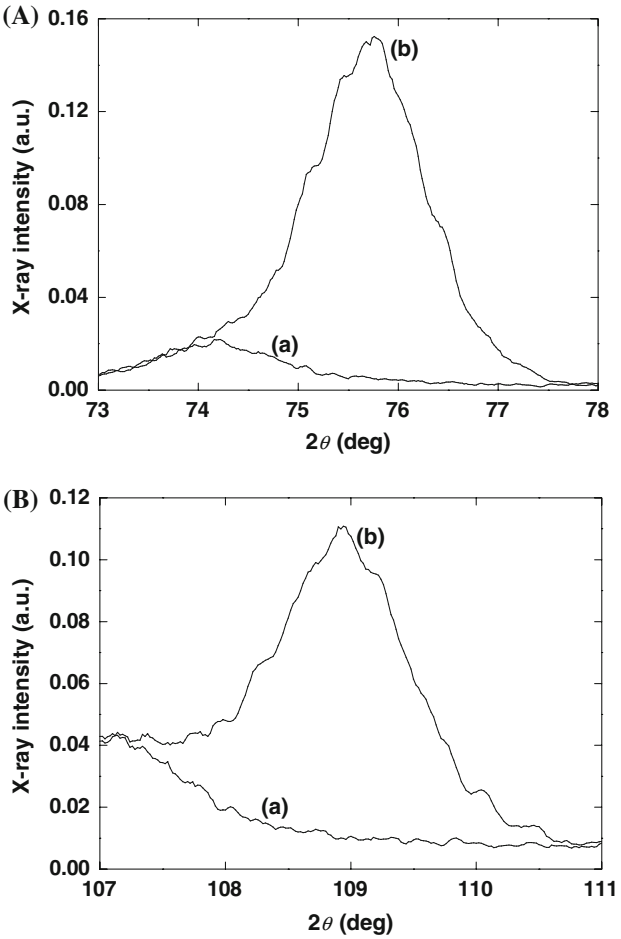

Fig. 2 XRF profiles of S atom (**A**) and Si atom (**B**): (a) YAG:Ce^{3+} nanoparticles, (b) MPTMS-modified YAG:Ce^{3+} nanoparticles

showing that the YAG:Ce^{3+} nanoparticles were modified with a few amount of MPTMS. Figure 3 shows the FT-IR spectrum of YAG:Ce^{3+} nanoparticles with and without MPTMS modification. The IR peak corresponding to the S–H stretching vibration mode was observed at 2565 cm^{-1} in the FT-IR spectrum of the MPTMS-modified YAG:Ce^{3+} nanoparticles [24]. Therefore, SH groups were introduced to the YAG:Ce^{3+} nanoparticles. The methoxy group of MPTMS is hydrolyzed by water of hydrate starting materials or water in air, and dehydrocondensed with OH groups on YAG:Ce^{3+} nanoparticles to form siloxane linkage [25].

Quantitative analysis of SH groups on the surface of YAG:Ce^{3+} nanoparticles

The above-mentioned methods analyze the SH groups on both the surface and the volume of nanoparticles. Therefore, Ellman method [23] is used as a quantitative analysis of freely accessible SH groups on the surface of YAG:Ce^{3+} nanoparticles. Since Ellman's reagent, DTNB, cannot

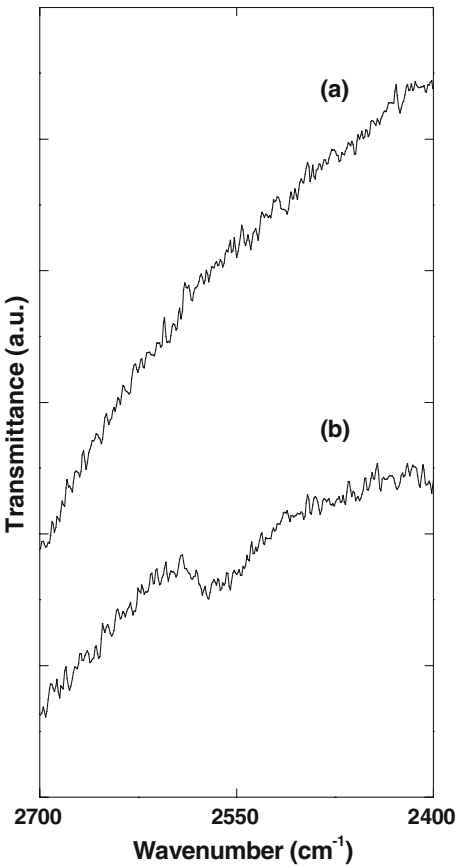

Fig. 3 FT-IR spectra of SH group: (a) YAG:Ce^{3+} nanoparticles, (b) MPTMS-modified YAG:Ce^{3+} nanoparticles

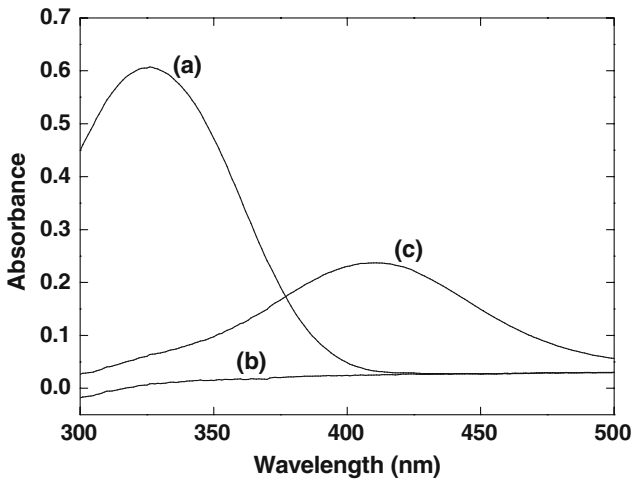

Fig. 4 Change in UV–vis spectra: (a) DTNB solution, (b) YAG:Ce^{3+} colloidal solution, (c) reaction between DTNB and MPTMS-modified YAG:Ce^{3+} colloidal solution

penetrate siloxane network, this method can quantify SH groups only on the surface. As shown in Fig. 4, the absorption peak of TNB was observed at 412 nm in the MPTMS-modified YAG:Ce^{3+} colloidal aqueous solution, whereas such a peak was not observed in DTNB solution

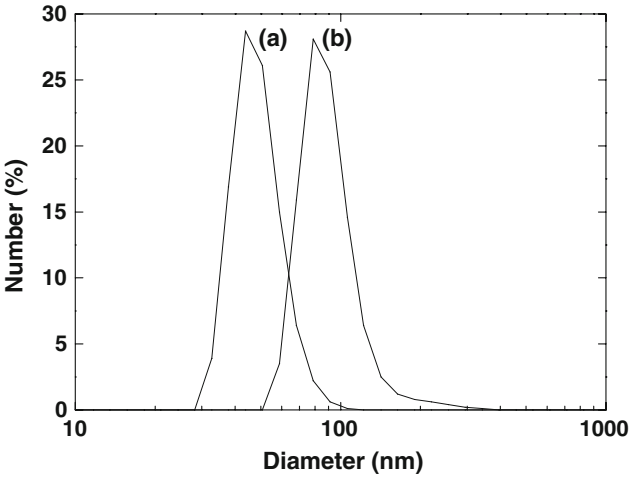

Fig. 5 Particle size distribution measured by DLS for YAG:Ce^{3+} nanoparticles diluted in ultra pure water (a) and MPTMS-modified YAG:Ce^{3+} nanoparticles diluted in ultra pure water (b)

and unmodified YAG:Ce^{3+} colloidal aqueous solution. This indicates that SH groups were introduced on the surface of the MPTMS-modified YAG:Ce^{3+} nanoparticles. Figure 5 shows the particle size distribution of YAG:Ce^{3+} nanoparticles with and without MPTMS modification measured by DLS. The mean particle size of the YAG:Ce^{3+} nanoparticles were 46 nm, while it has become 85 nm after MPTMS modification. This increase possibly results from not only the formation of hydrolyzed MPTMS shell, but also the formation of –Si–O–Si– bridging between the nanoparticles by polycondensation of hydrolyzed MPTMS. The number of SH groups per YAG:Ce^{3+} nanoparticle (diameters of $\sim$85 nm) was approximately 6.62×10^2, and the amount of MPTMS bound per unit surface area of the particle was approximately 9.52×10^{-6} g/m^2. This value is three orders of magnitude lower than 2.50×10^{-3} g/m^2 for ideal closed-packed MPTMS monolayer, assuming that the cross-sectional area of adsorbed MPTMS is 2.16 nm^2. Thus, MPTMS does not entirely cover the whole surface of the YAG:Ce^{3+} nanoparticles. This results from the following reasons: (i) MPTMS was completely dissolved in 1,4-BD because of less hydrolysis, (ii) a small number of OH groups are present on the surface of the YAG:Ce^{3+} nanoparticles, (iii) SH groups of MPTMS might be strongly covalently bound with surface metal atoms of the YAG:Ce^{3+} nanoparticles after their proton dissociation.

Fluorescence properties

Figure 6 shows the PL and PLE spectra of YAG:Ce^{3+} nanoparticles with and without MPTMS modification. No appreciable differences in the fluorescence intensity and spectral shape between both nanoparticles were recognized. It is well known that surface passivation plays a

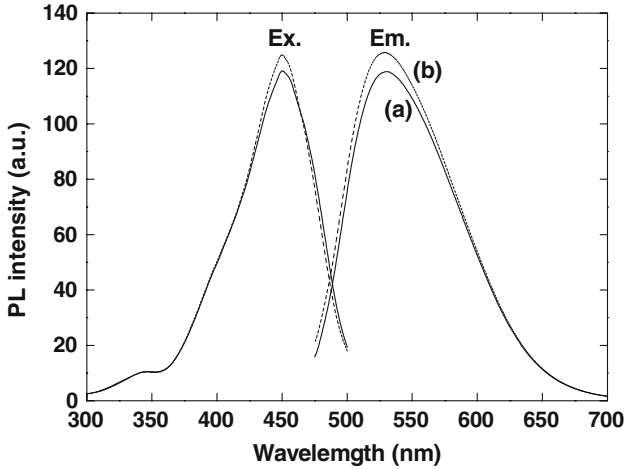

Fig. 6 PL and PLE spectra of YAG:Ce^{3+} colloidal aqueous solution (a) and MPTMS-modified YAG:Ce^{3+} colloidal aqueous solution. PL and PLE spectra were measured by monitoring the optimum wavelength, i.e. 450 and 530 nm, respectively

significant role in the improvement of fluorescence properties. However, in this work, the amount of bound MPTMS was not enough to cover the whole surface, and it was only partially dispersed on the surface, as already mentioned above. Accordingly, the fluorescence intensity does not change after MPTMS treatment. The excitation peaks are observed at 450 and 345 nm, the former is assigned to the 4f → 5d ($^2A_{1g}$) transition and the latter to the 4f → 5d ($^2B_{1g}$) transition for Ce^{3+} incorporated in YAG. The emission consists of overlaid peaks at 530 and ~570 nm. The former is assigned to the 5d ($^2A_{1g}$) → 4f ($^2F_{5/2}$) transition and latter to the 5d ($^2B_{1g}$) → 4f ($^2F_{7/2}$) transition for Ce^{3+} incorporated in YAG [22].

Demonstration of biological imaging

Avidin-immobilized agarose gel beads were stained by biotinylated-YAG:Ce^{3+} nanoparticles, as shown in Fig. 7a and b, while these beads were not tagged with MPTMS-modified YAG:Ce^{3+} nanoparticles without biotinylation. These results suggest that biotinylated-YAG:Ce^{3+} nanoparticles are successfully bound to the surface of the avidin-immobilized agarose gel beads through the selective avidin–biotin interaction. In addition, antirabbit IgG-immobilized YAG:Ce^{3+} nanoparticles are successfully bound to the surface of the rabbit IgG-immobilized agarose gel beads through the selective antibody–antigen interaction, as shown in Fig. 7c and d.

Conclusions

SH groups were introduced to YAG:Ce^{3+} nanoparticles prepared by glycothermal synthesis, followed by silanization at 65 °C for 6 h using MPTMS. The presence of SH groups was confirmed by XRF, FT-IR, and Ellman's method. Avidin-immobilized agarose gel beads were stained by biotinylated YAG:Ce^{3+} nanoparticles, whereas rabbit IgG-immobilized agarose gel beads were also stained

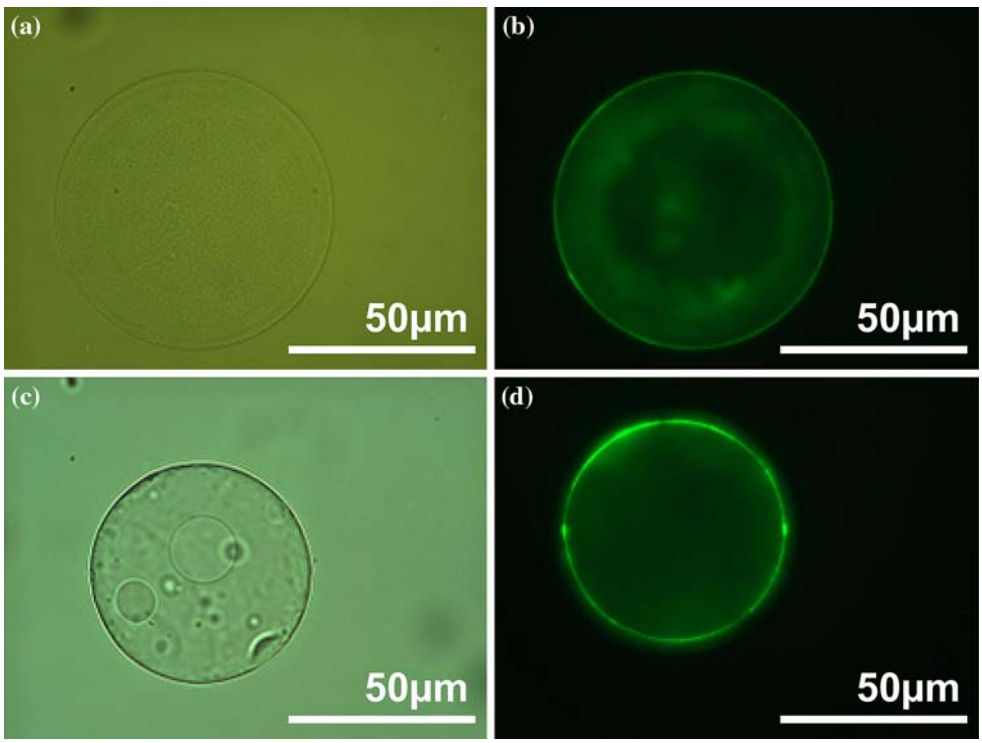

Fig. 7 Microscopic images of agarose gel beads: **a**, **b** treated with biotinylated-YAG:Ce^{3+} nanoparticles on avidin-immobilized agarose gel beads; **c**, **d** treated with antirabbit IgG-immobilized YAG:Ce^{3+} nanoparticles on rabbit IgG-immobilized agarose gel beads

by antirabbit IgG-immobilized YAG:Ce^{3+} nanoparticles. Thus, MPTMS-modified YAG:Ce^{3+} nanoparticles can conjugate with various biomolecules such as proteins and DNA, and can be used as a inorganic fluorescent probe for biological imaging.

References

1. Yang W, Zhang CG, Qu HY, Yang HH, Xu JG (2004) Anal Chim Acta 503:163. doi:10.1016/j.aca.2003.10.045
2. Trau D, Yang W, Seydack M, Caruso F, Yu NT (2002) Anal Chem 21:5480. doi:10.1021/ac0200522
3. Arya H, Kaul Z, Wadhwa R, Taira K, Hirano T, Kaul SC (2005) Biochem Biophys Res Commun 329:1173. doi:10.1016/j.bbrc.2005.02.043
4. Bruchez M Jr, Moronne M, Gin P, Weiss S, Alivisatos AP (1998) Science 281:2013. doi:10.1126/science.281.5385.2013
5. Mattoussi H, Mauro JM, Goldman ER, Anderson GP, Sundar VC, Mikulec FV, Bawendi MG (2000) J Am Chem Soc 122:12142. doi:10.1021/ja002535y
6. Murray CB, Norris DJ, Bawendi MG (1993) J Am Chem Soc 115:8706. doi:10.1021/ja00072a025
7. Gerion D, Pinaud F, Williams SC, Parak WJ, Zanchet D, Weiss S, Alivisatos AP (2001) J Phys Chem B 105:8861. doi:10.1021/jp0105488
8. Gaponik N, Talapin DV, Rogach AL, Hoppe K, Shevchenko EV, Kornowski A, Eychmuller A, Weller H (2002) J Phys Chem B 106:7177. doi:10.1021/jp025541k
9. Willman WY, Emmanuel C, Rebekah D, Vicki LC (2006) Biochem Biophys Res Commun 348:781. doi:10.1016/j.bbrc.2006.07.160
10. Sung JC, Dusica M, Manasi J, Beate R, Steffen H, Francois MW (2007) Langmuir 23:1974. doi:10.1021/la060093j
11. Müller J, Lupton JM, Rogach AL, Feldmann J (2004) Appl Phys Lett 85:381. doi:10.1063/1.1769585
12. Wijtmans M, Rosenthal SJ, Zwanenburg B, Poorter NA (2006) J Am Chem Soc 128:11720. doi:10.1021/ja063562c
13. Aldana J, Wang YA, Peng X (2002) J Am Chem Soc 123:8844. doi:10.1021/ja016424q
14. Celik A, Comelecoglu U, Yalin S (2005) Toxicol Ind Health 21:243. doi:10.1191/0748233705th237oa
15. Fischer B, Skreb Y (2001) Arh Hig Rada Toksikol 52:333
16. Bouden C, Damerval M (1982) Toxicol Eur Res 4:143
17. Kirchner C, Liedl T, Kudera S, Pellegrino T, Javier AM, Gaub HE, Stolzle S, Fertig N, Parak WJ (2005) Nano Lett 5:331. doi:10.1021/nl047996m
18. Abraham AW, Daniele G, Micha V, Jia S, Adam S, Shaowei C, Zhang JZ (2006) J Phys Chem B 110:5779. doi:10.1021/jp055058k
19. Kasuya R, Isobe T, Kuma H, Katano J (2005) J Phys Chem B 109:22126. doi:10.1021/jp052753j
20. Tomiki T, Akamine H, Gushiken M, Kinjoh Y, Miyazato M, Miyazato T, Toyokawa N, Hiraoka M, Hirata N, Ganaha Y, Futemma T (1991) J Phys Soc Jpn 60:2437. doi:10.1143/JPSJ.60.2437
21. Asakura R, Isobe T, Kurokawa K, Aizawa H, Ohkubo M (2006) Anal Bioanal Chem 386:1641. doi:10.1007/s00216-006-0814-6
22. Kasuya R, Isobe T, Kuma H (2006) J Alloy Compd 408–412:820. doi:10.1016/j.jallcom.2005.01.066
23. Ellman GL (1959) Arch Biochem Biophys 82:70. doi:10.1016/0003-9861(59)90090-6
24. Li Y-S, Wang Y, Tran T, Perkins A (2005) Spectrochim Acta A 61:3032. doi:10.1016/j.saa.2004.11.031
25. Shen X-C, Fang X-Z, Zhou Y-H, Liang H (2004) Chem Lett 33:1468. doi:10.1246/cl.2004.1468